Embracing the Chaos: Alloying Adds Stochasticity to Twin Embryo Growth

Yang Hu,[1] Vladyslav Turlo,[2] Irene J. Beyerlein,[3,4] Subhash Mahajan,[5] Enrique J. Lavernia,[1] Julie M. Schoenung,[1] and Timothy J. Rupert[1,2,*]

[1]*Department of Materials Science and Engineering, University of California, Irvine, California 92697, USA*
[2]*Department of Mechanical and Aerospace Engineering, University of California, Irvine, California 92697, USA*
[3]*Mechanical Engineering Department, University of California, Santa Barbara, California 93106, USA*
[4]*Materials Department, University of California, Santa Barbara, California 93106, USA*
[5]*Department of Materials Science and Engineering, University of California, Davis, California 95616, USA*

(Received 26 June 2020; revised 3 September 2020; accepted 8 October 2020; published 13 November 2020)

High-throughput atomistic simulations reveal the unique effect of solute atoms on twin variant selection in Mg-Al alloys. Twin embryo growth first undergoes a stochastic incubation stage when embryos choose which twin variant to adopt, and then a deterministic growth stage when embryos expand without changing the selected twin variant. An increase in Al composition promotes the stochastic incubation behavior on the atomic level due to nucleation and pinning of interfacial disconnections. At compositions above a critical value, disconnection pinning results in multiple twin variant selection.

DOI: 10.1103/PhysRevLett.125.205503

Mg-rich alloys are attractive engineering materials because of their unique properties, with a key example being high specific strength as compared to other metals. For example, while Al or Fe alloys are widely used as structural materials in aerospace and the automobile industry, replacing them with Mg alloys would significantly reduce the weight of aircraft and vehicles, as well as increase fuel efficiency [1,2]. However, Mg alloys tend to be brittle due to the limited number of easily activated dislocation slip systems in hexagonal close-packed (hcp) materials [3,4]. Therefore, twinning becomes an important deformation mode during the plastic deformation of Mg alloys, and the ductility or formability of Mg alloys can be improved via the formation of twin meshes (defined as two or more intersecting arrays of twins). For example, Lentz *et al.* successfully constructed double twin meshes in Mg-Li alloys, with the resultant sample achieving large compression failure strains (>30%) [5]. A more recent work by Wang *et al.* also showed that higher ultimate tensile strength and twofold increases in ductility was realized in pure Mg samples with gradient twin meshes consisting of intersecting $\{10\bar{1}2\}$ and $\{10\bar{1}1\}$ twins [6].

The formation of intersecting twin meshes requires the activation of multiple twin variants, which is usually explained based on high Schmid factor [7,8], local stress state [7,8], or minimization of the compatibility strain [9,10]. In contrast, the effect of alloying element additions is typically neglected. However, Cui *et al.* [11] reported deformed microstructures that contained significant differences between pure Mg and Mg-Al-Zn alloys, hinting that alloying can fundamentally change the twinning process. As shown in Fig. S1 in the Supplemental Material [12], the microstructure of the precompressed pure Mg, AZ31 (Mg-3.1Al-0.9Zn-0.45Mn, wt. %), and AZ91 (Mg-8.9Al-0.89Zn-0.42Mn, wt. %) samples show that there are more twins with smaller thicknesses in the alloy samples than the pure Mg sample that was deformed to the same extent. More importantly, there are increased numbers of twin variants being activated in the alloys than the pure Mg sample. The effect of solutes on twinning nucleation has been reported in Mg alloyed with rare earth elements [15,16], and reduced twin thickness has been observed in Mg alloys with solute segregation to the twin boundaries [17], but the effect of solute addition on twin variant selection has not been studied. Moreover, many studies on the growth mechanisms of mature twins in pure Mg and Mg alloys have been conducted, yet twin embryo growth mechanisms are largely neglected both experimentally and theoretically, despite the fact that the growth of twin embryos at early stages should influence the final twin morphology. For example, Luque *et al.* [18] and Spearot *et al.* [19] have described the growth of mature twins in deterministic ways using the idea that twin thickening occurs through the nucleation and propagation of disconnection loops or terraces. In these studies, twin boundary velocity (twin growth rate) was found to be a function of grain size, temperature, applied stress, and character of the disconnection loops nucleated on the twin plane (such as disconnection loop size, step height, etc.).

In the current study, molecular dynamics (MD) simulations of the early stages of twin embryo growth in Mg-Al alloys are used to isolate the effect of solute addition. A schematic of the triclinic simulation cell is shown in Fig. 1(a), with the x axis set along the $[1\bar{2}10]$ direction and the y axis set along the $[10\bar{1}1]$ direction. The top and bottom surfaces of the simulation cell are, therefore, parallel to the $(\bar{1}012)$ twin

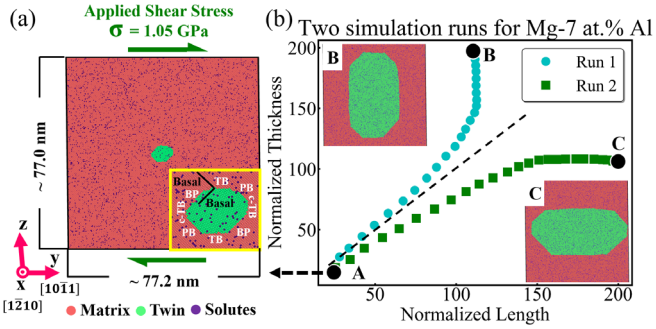

FIG. 1. (a) The atomic snapshot of the simulation box with the initial twin embryo shown. The inset of (a) shows an enlarged view of the twin embryo, and the basal planes in the matrix and the twin are marked using solid black lines. (b) The variation of normalized twin thickness with normalized twin length for two simulation runs of Mg-7 at. % Al. The insets of (b) show the final configurations of twin embryos in the two runs.

plane. The dimensions of the simulation box are approximately $5.1 \times 77.2 \times 77.0$ nm^3 in the x, y, and z directions with periodic boundary conditions being applied to all directions. The sample contains ~1300000 atoms. One twin embryo with a length of 7.6 nm and a thickness of 4.1 nm is inserted at the center of a simulation box using the Eshelby method reported by Xu *et al.* [20]. The inset of Fig. 1(a) shows the morphology of the twin embryo, which is bound by twin boundaries (TBs), conjugate TBs (c-TBs, almost 90° to the TBs), basal-prismatic (BP), and prismatic-basal (PB) interfaces. Al atoms are then introduced by randomly replacing Mg atoms, with the average concentration varying from 0–10 at. %. Note that the size of the simulation box for different alloy compositions was slightly different due to the change of equilibrium lattice constant as solute concentration was varied (see Fig. S3 in the Supplemental Material [12]).

MD simulations are conducted using the large-scale atomic/molecular massively parallel simulator (LAMMPS) package [21] and an embedded-atom method (EAM) potential developed by Liu *et al.* [22]. Shear deformation is applied to the simulation box to drive embryo growth. First, a global shear stress of around 1.05 GPa is applied to the simulation cell using an NPT (isothermal-isobaric) ensemble at 1 K. The cell is held for 1 ps, by which time any fluctuations in the shear stress have become negligible. After this time, an NVT (isothermal-isochoric) ensemble is then used to fix the shear strain value that was responsible for the ~1.05 GPa stress (varies slightly with alloy composition) and relax the simulation cell. We note that the twin embryo wants to grow to relax the applied stress, which results in a drop in global shear stress as the twin fraction increases (Fig. S7 [12]). For Mg-Al alloys, sixty samples with the same global concentration but different distribution of solutes are used to enable a statistical analysis of twinning. For pure Mg samples, sixty samples are also used but with different initial atomic velocity distributions. Visualization of atomic configurations are performed using the OVITO software [23], while the polyhedral template matching method [24] is used to characterize local crystalline structure and atomic orientation. Atoms in the matrix and twin are then differentiated from each other using this orientation information, with Mg atoms in the matrix colored red and those in the twinned region colored green. In all images, the Al solutes are colored dark purple. Details on the use of lattice orientation to differentiate twin from matrix are included in Sec. S2 of the Supplemental Material [12].

In our previous work on twin embryo growth in pure Mg [25], the lateral propagation of c-TBs was observed to be faster than the migration of TBs, which leads to TBs becoming the primary boundaries as the twin grows and matures. TB motion occurred by disconnection propagation, and a logarithmic relation between twin length and thickness was obtained. However, we observe here that these findings do not hold true and embryo growth in the alloy samples exhibits a very different growth behavior. Using Mg-7 at. % Al alloys as examples, Fig. 1(b) shows the evolution of twin embryos in two samples. We observe two different twinning behaviors, in which either the TB or c-TB becomes the primary boundary, leading to two different shapes. To follow the changes in shape, the twin length and thickness are measured as the position difference of the two TBs and c-TBs, respectively, with procedural details provided in Sec. S3 of the Supplemental Material [12]. To allow for a better comparison of twin embryo growth among the sixty alloy samples, the twin length and thickness are normalized by the lattice constant a at a given concentration. The black dashed line in Fig. 1(b) is the 1 : 1 reference line, so the samples with horizontally and vertically grown twin embryos exhibit data points above or below the reference line, respectively. We note that the data generated near the end of the simulation, namely, after the twin embryo reaches 22 vol. % of the simulation cell, is not used for any analysis due to the strong interaction with periodic images (see Sec. S4 of the Supplemental Material [12]).

The first suspected cause for the two distinct evolutions in embryos is the variations in local stress between different random samples since twin embryos grow towards regions with large shear stress. However, we find that there is no discernible difference in the initial stress state in these samples (see Sec. S5 of the Supplemental Material [12] for additional discussion), while the deviation in twinning behavior occurs at a very early growth stage. Thus, local stress variations are not the driving force for twin variant selection in our simulations.

To differentiate between the horizontally and vertically grown twin variants, it is convenient to use the aspect ratio (AR), which is defined here as a twin thickness divided by twin length. Analyzing the two examples shown in Fig. 1(b), the atomic positions of the twin embryos at 0.5 and 22 vol. % overlap for the horizontally grown embryo [Fig. 2(a)], while there are substantial deviations in atomic positions for the

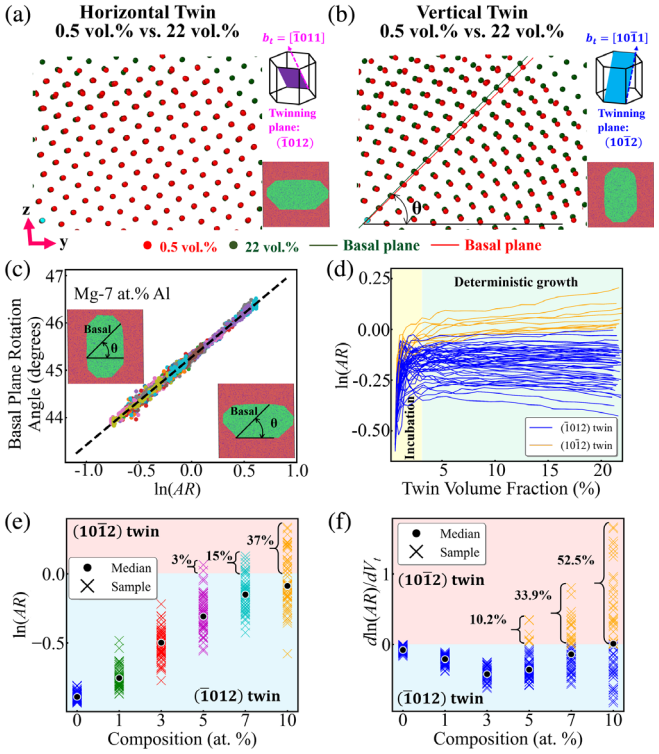

FIG. 2. The atomic positions of a twin embryo at the beginning (0.5 vol. %) and end (22 vol. %) of a simulation for (a) a sample which grows horizontally and has TBs as the primary boundaries and (b) a sample which grows vertically and has c-TBs as the primary boundaries. (c) Basal plane rotation angle versus the natural logarithm of aspect ratio for Mg-7 at. % Al samples, showing a linear relationship. (d) The variation of $\ln(AR)$ with twin volume fraction for Mg-7 at. % Al samples. (e) The natural logarithm of aspect ratio taken at the end of the simulations for pure Mg and Mg-Al alloy samples with different concentrations. The median of the data for each composition and the fraction of samples with $\ln(AR)$ larger than zero is also shown. (f) The average value of $d\ln(AR)/dV_t$ measured in the range from 15 to 22 vol. % in (e) is used to extrapolate to an infinitely large sample cell size.

vertically-grown embryo [Fig. 2(b)], indicating rotation of basal planes during vertical twin embryo growth. An additional example of this basal plane rotation is shown in Fig. S10 of the Supplemental Material [12]. Considering all simulation data, a linear dependence between the basal plane rotation angle (defined as the misorientation between the basal plane and the yz plane) and the natural logarithm of aspect ratio is revealed, as shown in Fig 2(c). The existence of this trend, as well as the analysis of experimental data (see Sec. S6 of Ref. [12]), identifies that the horizontally grown and vertically grown twins belong to different cozone twin variants, specifically the $(\bar{1}012)$ twin and $(10\bar{1}2)$ twin, corresponding to the negative and positive sign of $\ln(AR)$, respectively.

To understand the origins of the two states, we analyze the evolution of twin embryo shape using the variation of $\ln(AR)$ with the twin volume fraction (V_t), as shown in Fig. 2(d). Since the same initial embryo configuration is used for all samples, all of the curves start from the same negative value corresponding to the initial $(\bar{1}012)$ twin embryo. During the early growth stage, all of the curves strongly fluctuate up and down until they converge to either an increasing or decreasing trend, indicating the future twin variant. Eventually, as an indication of the two divergent behaviors, the value of $\ln(AR)$ becomes larger than 0 for some curves, indicating a transition to the $(10\bar{1}2)$ twin variant, while remaining below 0 for others. This analysis thus identifies two stages of twin embryo growth, a stochastic incubation stage and the deterministic growth stage, as denoted in Fig. 2(d).

The transition from one stage to another can be determined by tracking the slope $d\ln(AR)/dV_t$ for each curve (see Sec. S7 of the Supplemental Material [12]), where the sign of the slope shows the intent to adopt one twin variant or another. The twin volume fraction corresponding to the transition point increases with an increase in solute composition (Fig. S15 [12]), making the stochastic stage more prominent. In turn, the probability of adopting the $(10\bar{1}2)$ twin variant increases with increasing solute composition, as demonstrated in Fig. 2(e). In this figure, $\ln(AR)$ is obtained for each sample at the end of the simulation run (22 vol. %), and plotted for the sixty samples at each alloy composition. The median values of $\ln(AR)$ for each composition are marked with black dots and shift closer to 0, meaning that there is more random selection of twin variant at higher compositions. Our simulations had to be halted once the embryo approached the cell boundaries. Occasionally, an embryo was growing in a way such that it would eventually choose the alternative $(10\bar{1}2)$ variant, but was stopped prematurely while still in the expected $(\bar{1}012)$ variant.

To extrapolate our MD results to larger length scales and better determine the chances to adopt another twin variant, we calculated the average slope $d\ln(AR)/dV_t$ in the range from 15 to 22 vol. % for each sample and present them in Fig. 2(f). Again, values below 0 would correspond to the expected $(\bar{1}012)$ twin, while values above 0 would indicate selection of the alternative $(10\bar{1}2)$ variant. Consistent with results from direct simulation, the extrapolation to larger simulation sizes suggest that alloying Mg with >5 at. % Al should promote the formation of multiple twin variants. The exact critical solute concentration beyond which there is possibility of forming multiple twin variants may be influenced by the applied stress and temperature or even the limitations of the interatomic potential to capture all nuances of the Mg-Al system, but the existence of this critical concentration itself is unexpected and profound. The fact that alloying can overcome the typical strong preference believed to be predetermined by the relative orientation of the grain and applied stress has not been reported to date. Additional simulations were conducted to

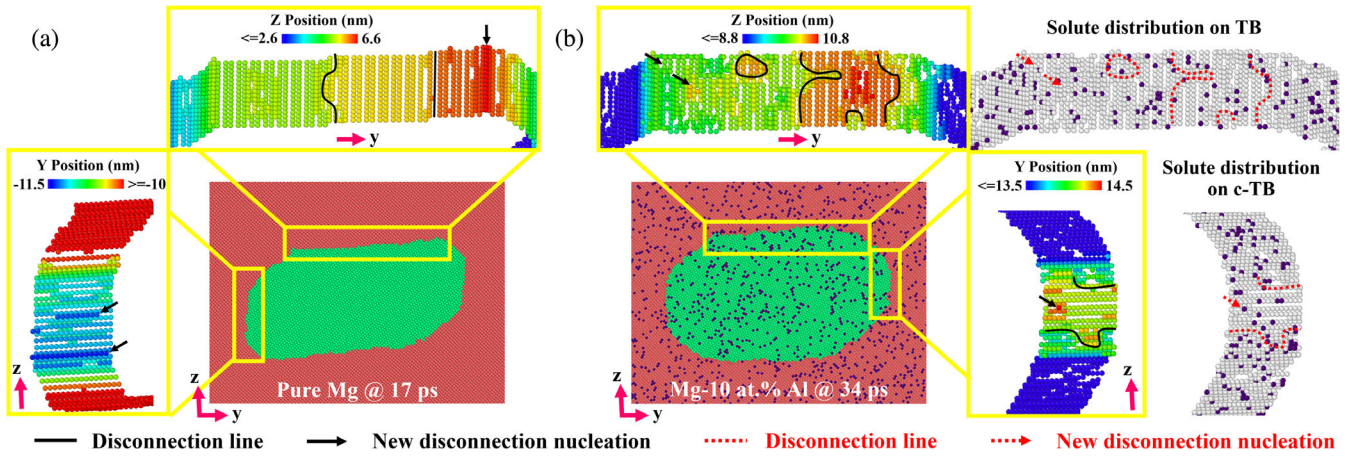

FIG. 3. Twinning disconnections formed on a TB and a c-TB in (a) pure Mg and (b) Mg-10 at. % Al samples. Atoms are colored using their Y positions in the enlarged views of c-TBs, while they are colored using their Z positions in the enlarged views of TBs. In (b), solute distribution on the TB and c-TB is also shown.

probe the effect of temperature, stress, initial embryo shape and alloying element type, with the results shown in Sec. S9 of the Supplemental Material [12]. In all cases, we observe multiple twin variant selection, proving that this behavior is widespread.

Stochastic selection of multiple twin variants opens a pathway for the formation of twin meshes within individual grains. On the one hand, when the same macroscopic stresses are applied, a grain in an alloyed sample is more likely to develop multiple twin variants than a grain in a pure Mg sample, which could then result in intersecting twins which started as different twin embryos. On the other hand, we find via our simulations that the addition of more solutes also slows the growth of the twin embryos, potentially even restricting growth completely (Fig. S18 and Fig. S19 of the Supplemental Material [12]). The critical solute composition for having multiple twin variants must be smaller than the one for completely restricting twin growth to have both (i) considerable twin embryo growth and (ii) the random selection of twin variant. This requirement provides a possible criterion to choose the appropriate solute types.

To reveal the atomistic mechanisms behind random twin variant selection in the high-concentration alloy samples, we focus on the effect of solute atoms on the nucleation and propagation of twinning disconnections, since these two processes drive the twin embryo growth [25]. Twinning disconnections are defined as interfacial dislocations with step character and account for the formation and migration of TBs [26–28]. In our simulations, twinning disconnections can be nucleated in two ways, depending on the source of disconnection nucleation. As shown in Fig. 3(a), twinning disconnections are formed at BP/PB interfaces in pure Mg samples, which then migrate towards each other to advance the TB or c-TB. The black arrows mark the formation of new twinning disconnections, while solid black lines mark disconnection lines. Solute atoms have both supportive and restrictive impacts on embryo growth. On the one hand, solute atoms promote the nucleation of twinning disconnections at the TBs or c-TBs themselves [18,29,30]. In the alloy sample shown in Fig. 3(b), small disconnection loops (circled in black) have nucleated in the middle of the TB, indicating homogeneous nucleation of twinning disconnections without the assistance of the BP/PB interfaces. On the other hand, solutes exhibit a pinning effect and can reduce the velocity of twinning disconnection motion [18,29,30]. Disconnection lines in the alloy samples are more tortuous than the disconnection lines in pure Mg samples because of this pinning effect of solutes. While similar findings of solute effect on the nucleation and propagation of twinning disconnections during the growth of mature twins can be found in Refs. [18,29,30], our work further reveals that solute atoms also dramatically influence twin embryo growth. In Sec. S10 of the Supplemental Material [12], we show the velocity of TBs and c-TBs due to the interplay of disconnection nucleation and propagation for different alloys. In pure Mg samples, the c-TBs move much faster than TBs, corresponding to the formation of horizontally grown $(\bar{1}012)$ twins. As the solute concentration increases, the motion of c-TBs becomes slower and, at a certain concentration level, the pinning effect of solutes is strong enough to induce the possibility of forming the vertically grown $(10\bar{1}2)$ twins. For a given individual embryo, the stochastic events of disconnection nucleation and pinning or unpinning lead to either higher TB velocity or higher c-TB velocity within an early stage of twin embryo growth, corresponding to the stochastic selection of different twin variants. This velocity difference will then maintain during the following deterministic growth stage, where there is embryo expansion without changing twin variant. BP/PB migration in a bicrystal geometry was also studied and confirmed that solutes slow the migration of

these interfaces (see Sec. S11 of the Supplemental Material [12]).

In summary, using atomistic simulations, we have discovered a process of random variant selection between $(\bar{1}012)$ and $(10\bar{1}2)$ co-zone twins in Mg-Al alloys after Al concentration reaches 5 at. % for the simulation geometry used here. The twin embryo growth can be separated into two stages: (i) the stochastic incubation stage when embryos choose which twin variant to eventually adopt, and (ii) the deterministic growth stage when embryos expand without changing the selected twin variant. The stochastic twin variant selection is caused by the stochastic events of nucleation and pinning or unpinning of twinning disconnections by solute atoms. These findings reveal a previously unknown effect of alloying on twinning and thereby benefit continuously emerging strategies for improving Mg properties via alloy design. We also note that this stochastic twin variant selection could be used for the construction of twin meshes. Forming twin meshes requires twins that grow in different directions and intersect each other, which can be accomplished by random twin variant selection in Mg alloys even for the same macroscopic stress state.

This research was supported by the National Science Foundation through Grants No. CMMI-1729829, No. CMMI-1729887, and No. CMMI-1723539.

*Corresponding author.
trupert@uci.edu

[1] W. J. Joost, in *Targeting High Impact R&D for Automotive Magnesium Alloys* (Springer, New York, 2017), p. 5.
[2] H. Dieringa, N. Hort, D. Letzig, J. Bohlen, D. Höche, C. Blawert, M. Zheludkevich, and K. U. Kainer, in *Mg Alloys: Challenges and Achievements in Controlling Performance, and Future Application Perspectives* (Springer, New York, 2018), p. 3.
[3] B. L. Mordike and T. Ebert, Magnesium: Properties—applications—potential, Mater. Sci. Eng. A **302**, 37 (2001).
[4] G. S. Rohrer, *Structure and Bonding in Crystalline Materials* (Cambridge University Press, Cambridge, England, 2001).
[5] M. Lentz, M. Risse, N. Schaefer, W. Reimers, and I. J. Beyerlein, Strength and ductility with $\{10\bar{1}1\}$—$\{10\bar{1}2\}$ double twinning in a magnesium alloy, Nat. Commun. **7**, 11068 (2016).
[6] X. Wang, L. Jiang, C. Cooper, K. Yu, D. Zhang, T. J. Rupert, S. Mahajan, I. J. Beyerlein, E. J. Lavernia, and J. M. Schoenung, Toughening magnesium with gradient twin meshes, Acta Mater. **195**, 468 (2020).
[7] L. Capolungo, P. E. Marshall, R. J. McCabe, I. J. Beyerlein, and C. N. Tome, Nucleation and growth of twins in Zr: A statistical study, Acta Mater. **57**, 6047 (2009).
[8] I. J. Beyerlein, L. Capolungo, P. E. Marshall, R. J. McCabe, and C. N. Tome, Statistical analyses of deformation twinning in magnesium, Philos. Mag. **90**, 2161 (2010).
[9] M. R. Barnett, Z. Keshavarz, A. G. Beer, and X. Ma, Non-Schmid behaviour during secondary twinning in a polycrystalline magnesium alloy, Acta Mater. **56**, 5 (2008).
[10] C. F. Guo, R. L. Xin, C. H. Ding, B. Song, and Q. Liu, Understanding of variant selection and twin patterns in compressed Mg alloy sheets via combined analysis of Schmid factor and strain compatibility factor, Mat. Sci. Eng. A **609**, 92 (2014).
[11] Y. J. Cui, Y. P. Li, Z. C. Wang, X. Ding, Y. Koizumi, H. K. Bian, L. Y. Lin, and A. Chiba, Impact of solute elements on detwinning in magnesium and its alloys, Int. J. Plast. **91**, 134 (2017).
[12] See Supplemental Material at http://link.aps.org/supplemental/10.1103/PhysRevLett.125.205503 for additional simulation details and experimental support, which includes Refs. [13,14].
[13] C. Lou, X. Y. Zhang, G. L. Duan, J. Tu, and Q. Liu, Characteristics of different $\{10\bar{1}2\}$ twin variants in magnesium alloy during room temperature dynamic plastic deformation, J. Mater. Res. **28**, 1885 (2013).
[14] https://sites.google.com/site/eampotentials/Home/MgY
[15] K. Hantzsche, J. Bohlen, J. Wendt, K. U. Kainer, S. B. Yi, and D. Letzig, Effect of rare earth additions on microstructure and texture development of magnesium alloy sheets, Scr. Mater. **63**, 725 (2010).
[16] C. J. Silva, A. Kula, R. K. Mishra, and M. Niewczas, Grain growth kinetics and annealed texture characteristics of Mg-Sc binary alloys, J. Alloy Compd. **687**, 548 (2016).
[17] J. F. Nie, Y. M. Zhu, J. Z. Liu, and X. Y. Fang, Periodic segregation of solute atoms in fully coherent twin boundaries, Science **340**, 957 (2013).
[18] A. Luque, M. Ghazisaeidi, and W. A. Curtin, A new mechanism for twin growth in Mg alloys, Acta Mater. **81**, 442 (2014).
[19] D. E. Spearot, L. Capolungo, and C. N. Tome, Shear-driven motion of Mg $\{10\bar{1}2\}$ twin boundaries via disconnection terrace nucleation, growth, and coalescence, Phys. Rev. Mater. **3**, 053606 (2019).
[20] B. Xu, L. Capolungo, and D. Rodney, On the importance of prismatic/basal interfaces in the growth of $(\bar{1}012)$ twins in hexagonal close packed crystals, Scr. Mater. **68**, 901 (2013).
[21] S. Plimpton, Fast parallel algorithms for short-range molecular dynamics, J. Comput. Phys. **117**, 1 (1995).
[22] X. Y. Liu, P. P. Ohotnicky, J. B. Adams, C. L. Rohrer, and R. W. Hyland, Anisotropic surface segregation in Al-Mg alloys, Surf. Sci. **373**, 357 (1997).
[23] A. Stukowski, Visualization and analysis of atomistic simulation data with OVITO–the Open Visualization Tool, Model. Simul. Mater. Sci. Eng. **18**, 015012 (2010).
[24] P. M. Larsen, S. Schmidt, and J. Schiøtz, Robust structural identification via polyhedral template matching, Model. Simul. Mater. Sci. Eng. **24**, 055007 (2016).
[25] Y. Hu, V. Turlo, I. J. Beyerlein, S. Mahajan, E. J. Lavernia, J. M. Schoenung, and T. J. Rupert, Disconnection-mediated twin embryo growth in Mg, Acta Mater. **194**, 437 (2020).
[26] J. Wang, J. Hirth, and C. Tomé, $(\bar{1}012)$ twinning nucleation mechanisms in hexagonal-close-packed crystals, Acta Mater. **57**, 5521 (2009).

[27] A. Ostapovets and R. Gröger, Twinning disconnections and basal–prismatic twin boundary in magnesium, Model. Simul. Mater. Sci. Eng. **22**, 025015 (2014).

[28] J. Hirth, J. Wang, and C. Tomé, Disconnections and other defects associated with twin interfaces, Prog. Mater. Sci. **83**, 417 (2016).

[29] M. Ghazisaeidi, L. G. Hector, and W. A. Curtin, Solute strengthening of twinning dislocations in Mg alloys, Acta Mater. **80**, 278 (2014).

[30] P. Yi and M. L. Falk, Thermally activated twin thickening and solute softening in magnesium alloys–a molecular simulation study, Scr. Mater. **162**, 195 (2019).